**ISSN** 1746-7659, England, UK
**Journal of Information and Computing Science**
Vol. 17, No. 1, 2022, *pp*.019-027

# Development of south Atlantic subtropical dipole and its relationship with ENSO

Liu Xueli, Dong Ran, Guo Chenguang, Li Yuxin
School of mathematics and statistics, Nanjing University of Information Science & Technology,
Nanjing 210044, China

(Received October 12, 2021, accepted January 29, 2022)

**Abstract:** Based on the monthly sea surface temperature (SST) data provided by Hadley Centre , the characteristics of Southern Subtropical Atlantic SST variation and its relationship with ENSO are discussed. The results of this paper show that: 1) In the summer of the southern hemisphere, the SST anomaly (SSTA) of the Southern Subtropical Atlantic presents a southwest-northeast antiphase dipole modes, that is, the South Atlantic Subtropical Dipole (SASD), which develops from September to November. It reaches its peak in austral summer(December January February ,the next year), weakens from March to May (the next year), and declines until austarl winter(June July August, the next year). 2) SASD is significantly correlated with ENSO, and positive SASD and negative SASD are correlated with El Niño and La Niña events respectively.

**Key words:** the South Atlantic Subtropical Dipole; ENSO; empirical orthogonal function; Composite analysis

## 1. Introduction

The ocean accounts for about 71% of the earth surface area and it is an important component that cannot be ignored in the global climate system. Ocean-atmosphere interaction is also an indispensable direction for studying the influence of the ocean on climate change[1]. The Atlantic is the second largest ocean and also the ocean with the largest latitude span. The entire basin is roughly "S" shaped. In an effort to understand the interannual variation of SST in the South Atlantic, Zhuang Hui et al.[2] showed that in the recent 140 years, the SST in the South Atlantic increases linearly at a significant annual rate of 0.0045℃ as a whole, and the SST in this area does not change significantly from 1870 to 1930. Venegas et al.[3] discussed the SST anomalies(SSTAs) for the first time in 1996. Morioka et al.[4] also pointed out that the Sea Surface Temperature Anomaly of the South Atlantic has an obvious spatial dipole mode, namely the South Atlantic Subtropical Dipole (SASD), and the locking season is austral summer. The mechanism of SASD formation is explained by discussing the variation of subtropical anticyclone, latent heat flux and mixed layer depth anomaly.

ENSO originates in the Tropical Pacific Ocean and oscillates between warm and cold with a period of 3~7 years[5]. It can have a significant impact on global weather converts through changes in the convection mode in the tropical Pacific[6-7]. The interaction between the atmosphere and the ocean in the tropical Pacific Basin plays an important role in defining the characteristics of ENSO[8], and many studies were also devoted to the relationship between ENSO and other tropical or subtropical oceans. Wu and Kug et al.[9-10] found that SST in the tropical Indian Ocean affects ENSO by regulating walker circulation in the Pacific and Indian Ocean in its coupling simulation.

Annamalai et al.[11] showed that the SSTAs in the Indian Ocean enhances the abnormal anticyclone generated in the northwest Pacific Ocean during the El Niño mature stage. By activating this anticyclonic mode, the east wind stress in the western Pacific Ocean is abnormal, and the warming of SST in the Indian Ocean leads to a faster transition to La Niña. Izumo et al.[12] also proposed that tropical Indian Ocean Dipole (IOD) events may contribute significantly to the long-term predictability of ENSO. Recently, Wang Lijuan et al.[13] proposed that there is a significant negative correlation between the South Indian Ocean Dipole and ENSO events. Fauchereau et al.[14] proposed that the SASD positive event is caused by the enhancement and southward movement of the South Atlantic subtropical high. Penland and Matrasova[15-16] found that the South Atlantic SST precedes the El Niño signal by 9 months using a linear inverse model. Wang[17] believed that the tropical Atlantic forces the equatorial Pacific through the interbasin SST gradient changes associated with the Walker circulation in the Atlantic. Jansen et al.[18] also came to similar conclusion. However, there are few studies on the relationship between the South Atlantic subtropical SST and ENSO.

In view of this, this paper will further explore the characteristics and development process of SASD and its relationship with ENSO. The South Atlantic Subtropical Dipole is expected to be further understood.

# 2. Data and methods

## 2.1 Data Description

SST data are based on global monthly average data provided by the Hadley Centre. The spatial resolution of data is 1° × 1°. The data were selected from January 1979 to December 2021.

Let $X_{amij}$ is data of a certain grid point, where $a$ is year, $a \in \{1979, 1980, \cdots\cdots, 2021\}$, a total of 43 years. $m$ represents months, $m \in \{1, 2, \cdots\cdots, 12\}$; $i$ represents longitude, $j$ represents latitude. The longitude we selected here ranges from 60°W to 20°E and the latitude ranges from 45°S to 15°N.

The first step was to calculate the seasonal climate state, such as the calculation formula of the seasonal climate state of a certain grid point:

$$\bar{X}_{ij} = \frac{\sum_{a=1979}^{2021} \frac{1}{3} \sum_{m} X_{amij}}{n} . \quad (1)$$

The second step was to calculate the seasonal average, and then use the seasonal average to remove the corresponding seasonal climate state data to obtain the annual seasonal average outliers.

$$\bar{X}_{aij} = \frac{\sum_{a} \sum_{m} X_{amij}}{3} . \quad (2)$$

$$X_{aij} = \bar{X}_{aij} - \bar{X}_{ij} . \quad (3)$$

Finally, the linear trend was removed by least square method to avoid the influence of global warming trend on the research results. Then the annual SSTAs of the austral summer in 43 years are obtained. The Niño3.4 Index used in this paper was treated in the same way.

## 2.2 Analysis method

### 2.2.1 Empirical orthogonal function decomposition

Empirical Orthogonal Function (EOF)[19-20] is widely used in the analysis of meteorological and Marine data. The function is to identify the main mutually orthogonal spatial distribution patterns from the dataset of meteorological element variables. In practical application, the field sequence of certain elements is decomposed into the sum of the product of orthogonal space function and orthogonal time function, that is,

$$X_{ij} = \sum_{h=1}^{H} T_{ih} \times V_{hj} = T \cdot V \quad (4)$$

In which, $X_{ij}$ is the SSTA values, $i = 1, 2, \cdots, m$ is the time serial numbers, $j = 1, 2, \cdots, n$ represents different stations, $T_{ih}$ is the function of time, $V_{hj}$ is the function of space, $h = 1, 2, \cdots, H$ represents the number of decomposition fields.

A spatial function is only a function of space, and it changes completely with space and not with time. The time function that only changes with time can be regarded as the weight coefficient of the typical field. In general, EOF converges quickly. The first few typical fields can roughly represent the situation of the actual field, and the change of the time coefficient corresponding to each typical field reflects the importance of each typical field at different moments.

This decomposition requires orthogonality, that is

$$V^T V = I, \quad I \text{ is the identity matrix.} \quad (5)$$

Time weight coefficients are also required to be orthogonal:

$$T \cdot T^T = \Lambda = \begin{bmatrix} \lambda_1 & & & \\ & \lambda_2 & & \\ & & \ddots & \\ & & & \lambda_m \end{bmatrix}. \quad (6)$$

### 2.2.2 Other analysis methods

After discussing the modes of SASD, we use the method of composition analysis[21] to discuss the evolution of SASD modes. In addition, correlation analysis was used to explore the relationship between SASD mode and ENSO, and statistical significance test was carried out.

(1) Correlation analysis

Correlation analysis is one of the commonly used statistical methods in meteorology, which can measure the relationship between two meteorological elements.

Suppose there are two variables, $x_1, x_2, \cdots\cdots, x_n$ and $y_1, y_2, \cdots\cdots, y_n$. The calculation formula of the correlation coefficient of these two variables is as follows:

$$r_{xy} = \frac{\sum_{i=1}^{n}(x_i - \bar{x})(y_i - \bar{y})}{\sqrt{\sum_{i=1}^{n}(x_i - \bar{x})^2}\sqrt{\sum_{i=1}^{n}(y_i - \bar{y})^2}}. \quad (7)$$

Where, $\bar{x},\bar{y}$ is the sample mean and $n$ is the sample size. The value of the correlation coefficient is between -1 and 1. When the correlation coefficient is positive, it indicates that there is a positive correlation between the two and their change trend is consistent. When the correlation coefficient is negative, it indicates that the two are negatively correlated and the change trend is opposite. When the absolute value of correlation coefficient is larger, the relationship between them is closer.

(2) Student T - test

According to the correlation coefficient $r \neq 0$ of n pairs of samples, whether they can be considered as the population correlation coefficient $\rho \neq 0$ between them，which needs to be statistically tested. The test method of whether the population correlation coefficient $\rho = 0$ depends on T test method of T distribution and U test method of normal distribution. The T test method is more commonly used at present. T test is suitable for mean test with unknown variance and data subject to normal distribution, even for small samples.

The calculation formula of the T-statistic of the test population mean is as follows:

$$t = \frac{\bar{x} - u_0}{s}\sqrt{n} \ . \tag{8}$$

Where, $\bar{x}$ and $s$ respectively represent the sample mean and standard deviation, $u_0$ is the population mean, and $n$ is the sample size. After the significance level $a$ is determined, the T-distribution table is checked according to the degrees of freedom $\lambda = n-1$. If $|t| > t_a$, the null hypothesis is rejected and significant changes are considered. Otherwise, the null hypothesis is accepted and the change is not significant.

# 3. Temporal and spatial distribution of the South Atlantic Subtropical Dipole

## 3.1 The spatial distribution of SASD

In order to understand the characteristics of the SST of the southern subtropical Atlantic in summer, we analyzed the SSTAs in December, January and February (DJF) of the South Atlantic basin (15°N~45°S, 60°W~20°E) by EOF. Fig.1 shows the spatial distribution of the first mode of EOF analysis, which is manifested by a strong SST gradient of the southwest region to the northeast region. And the variance contribution rate of the first mode is 35.58%. The SST distribution of this anti-phase was called the SASD[22], which is consistent with the results of previous studies[3-4]. There are significant positive anomalies in the northeast region of the dipole and the center is approximately 15°S~24°S, 24°W~3°W, which is called the NorthEast Pole (NEP). The SSTA center in the southwest region is approximately in 33°S~41°S, 28°W~6°W with negative anomaly distribution, which is called the SouthWest Pole (SWP)[23].

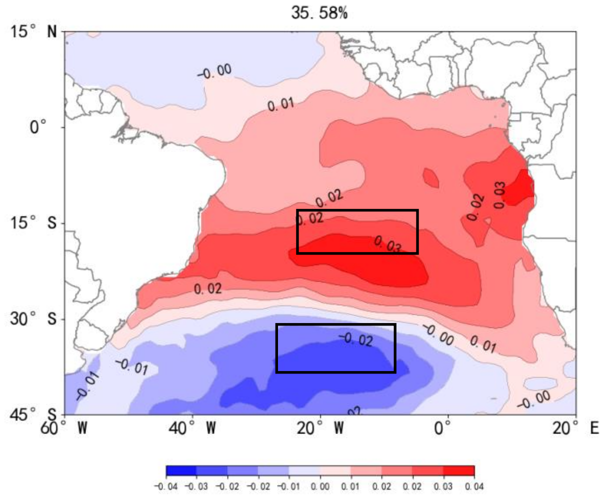


**Fig. 1** Spatial structure of the 1st EOF modes of the seasonally averaged observed SSTAs in the austral summer (DJF) from 1979 to 2021 in the Atlantic Ocean. The number(35.58%) at the upper center gives the percentage of total variance explained by the mode, and the contour intervals are 0.01°C

### 3.2 the seasonal evolution of SASD

In order to analyze the temporal and spatial distribution and evolution characteristics of SASD modes, major SASD events were composed by season in this section. Fig.2 shows the composition of major positive and negative SASD events in spring, summer, autumn and winter in the Southern Hemisphere. The results show that: In the composition of positive event years (Fig. 2 (a~d)), SSTAs gradually appeared in the region of the south Atlantic subtropical in the austral spring (September October November; SON). The positive SSTAs extended eastward from 20°S to 32°S in South America to the coast of west Africa, and no obvious maximum region of SSTAs appeared. The negative SSTAs were mainly concentrated between 30°S and 45°S, and the anomalies were small. After spring, the dipole mode continued to develop and reached the peak in austral summer (December January February; DJF). There were obvious positive and negative anomalies in SST, and the maximum positive SSTA reached 0.67 ℃. Then the positive SSTA gradually diffused westward from the northeast Pole. The intensity of SSTAs was also relatively weak. After the austral autumn (March April May; MAM), the dipole mode gradually collapse. The results of the negative events composite analysis (Fig.2 (e~h)) were similar to the development process of positive events, except that the negative dipole collapsed more slowly after the austral summer than the positive dipole. However, the intensity of the negative SSTA was greater than the positive dipole events during the summer peak. It can be seen that seasonal phase locking is an important characteristic of SASD mode.

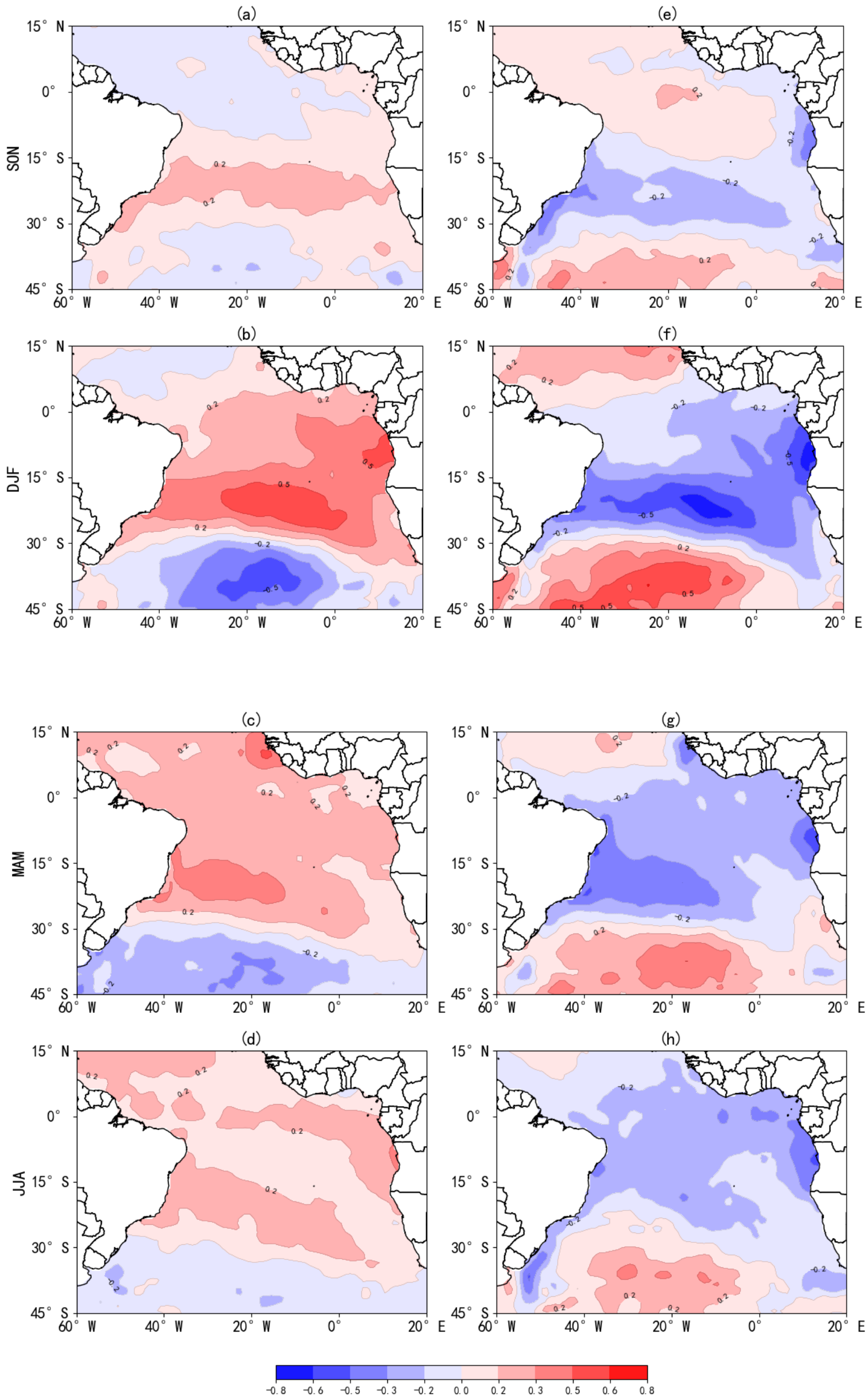


**Fig.2** Composite SSTA of positive events during austral spring(SON) (a), austral summer (DJF) (b), austral autumn (MAM) (c), and austral winter(JJA) (d). Composite SSTA of negative events during austral spring(SON) (e), austral summer (DJF) (f), austral autumn (MAM) (g), and austral winter(JJA) (h) (unit: ℃)

## 4. the relationship between SASD and ENSO

As the strongest signal of global Ocean-atmosphere interaction, ENSO can not only directly cause the abnormal weather and climate in the tropical Pacific, but also indirectly affect the weather and climate in the Indian And Atlantic Oceans and even around the world[7-8]. Therefore, ENSO will also make a certain contribution to SACZ precipitation. In order to understand the influence of the SASD on SACZ precipitation, this section analyzes the relationship between SASD and ENSO. Fig. 3 shows the time series PC1 (solid blue curve) of the first mode of SSTAs EOF analysis, and the solid red curve is Nino3.4 index (mean SSTAs of region 5°S~5°N, 170°W~120°W). According to the threshold selection method of existing literature[24-25], 0.6 standard deviation is used as the threshold value to select the years of major positive and negative dipole events ( shortened to as "positive event" and "negative event"): if PC1 is greater than 0.6 in the austral summer, it is called a positive event year; Conversely, PC1 less than -0.6 is said to be negative event year. That is, during the positive events, the NEP is positive SSTA, while the SWP is negative SSTA. On the contrary, when there is a negative anomaly in the NEP and a positive anomaly in the SWP, it is a negative SASD event. According to Fig.3, from 1979 to 2021, SASD positive event years were: 1982, 1983, 1985, 1987, 1994, 1997, 2002, 2004, 2009, 2015, 2018 and 2019, a total of 12 positive event years. Negative event years were: 1979, 1980, 1981, 1989, 1996, 2001, 2010, 2011, 2017, 2020, a total of 10 event years (we define the year of December ( D) as the year in which the dipole events occur). At the same time, according to the Oceanic Niño Index (ONI, https://ggweather.com/enso/oni.htm), we selected the years of the medium, strong and very strong El Niño (La Niña) events as the El Niño (La Niña) years and ignored the weak El Niño(La Niña) years. The results showed that there were seven El Niño years in positive SASD years (1982, 1987, 1994, 1997, 2002, 2009 and 2015), and no El Niño years in negative SASD years. However, there were three La Niña years in negative SASD event years (2010, 2011 and 2020), and no La Niña years in positive SASD event years. The specific years of each event are shown in Table 1, which also indicates that SASD events and ENSO events are in phase to a certain extent. Positive and negative SASD events correspond to positive (El Niño) and negative (La Niña) ENSO events respectively. Further, the correlation coefficient between PC1 and Niño3.4 index is 0.54, which passed 99% significance test. It can be seen that the SASD is strongly correlated with ENSO.

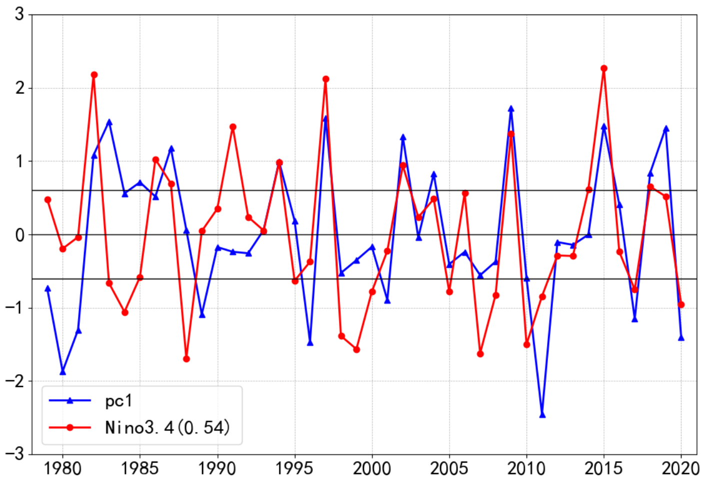


**Fig. 3** The principal component of the 1st EOF mode (PC1) for SSTAs in DJF (solid blue curve), and the Niño3.4 index (SSTAs averaged within 5°S~5°N, 170°W~120°W, units: ℃; solid red curve). The abscissa marks the years when a DJF season starts. PC1 is standardized to have unit SD, the values of the two black lines are 0.6 SD, and the number in brackets is the correlation coefficient between PC1 and the Niño3.4 index, And passes the 99% significance test

Tab.1 Years with positive and negative SASD events

| events | years |
|---|---|
| Positive events | 1982+，1983，1985，1987+，1994+，1997+，2002+，2004，2009+、2015+、2018,2019 |
| Negative events | 1979，1980，1981，1989，1996，2001，2010-，2011-，2017，2020- |

+ : El Niño events; − : La Niña events.

## 5. Conclusion

This paper discusses the characteristics of SST variation in southern subtropical Atlantic and its relationship with ENSO by analyzing the monthly SST data provided by Hadley Centre. The main conclusions are as follows:

1) In the austral summer, the South Atlantic SSTAs present an inverse phase distribution from southwest to northeast, namely SASD. This mode is an inherent feature of subtropical SSTAs in the South Atlantic. The formation of this mode has obvious seasonal characteristics.

2) The SASD mode is significantly correlated with ENSO. Their correlation coefficient was 0.54, which passed 99% significance test. The positive SASD and negative SASD events are correlated with El Niño and La Niña events respectively, and there is no cross correlation between them.

### References

[1] Ma Liping, Wang Panxing, Wu Hongbao. Regional differences of air-sea interactions in tropical oceans[J]. Journal of the Meteorological Sciences, 2001, 21(3): 260-270.

[2] Zhuang Hui, Zheng Chongwei, Jia Benkai, et al. South Atlantic Ocean Sea surface temperature characteristics analysis[J]. Journal of Yanbian University (Natural Science Edition), 2013, 39(02): 153-156.

[3] Venegas S, Mysak L A, Straub D N. Evidence for interannual and interdecadal climate variability in the South Atlantic[J]. Geophysical Research Letters, 1996, 23(19): 2673-2676.

[4] Morioka Y, Tozuka T, Yamagata T. On the growth and decay of the subtropical dipole mode in the South Atlantic[J]. Journal of Climate, 2011, 24(21): 5538-5554.

[5] Chang P. Climate fluctuations of tropical coupled systems—the role of ocean dynamics[J]. Journal of Climate, 2006, 19(20): 5122-5174.

[6] Ren Fumin, Yuan Yuan, Sun Chenghu, et al. Review of Progress of ENSO Studies in the PastThree Decades[J]. Advances in Meteorological Science and Technology, 2021, 2(3): 17-24.

[7] Wen Tao, Feng Licheng, Chen Quanliang, et al. Different influence on ENSO caused by East Asian Winter Minsoon and North Pacific Oscillation[J]. Journal of Applied Oceanography, 2021, 40(03): 373-381.

[8] Feng Junqiao, Lu Yunlong, Guan Cong, et al. Influence of subtropical Pacific variability on ENSO: Review and advance[J]. Marine Sciences, 2020, 44(8): 1-7.

[9] Wu R G, Kirtman B P. Understanding the impacts of the Indian Ocean on ENSO variability in a coupled GCM[J]. Journal of Climate, 2004, 17(20): 4019-4031.

[10] Kug J S, Kirtman B, Kang I S. Interactive feedback between ENSO and the Indian Ocean in an interactive ensemble coupled model[J]. Journal of Climate, 2006, 19(24): 6371-6381.

[11] Annamalai H, Xie S P, McCreary J P, et al. Impact of Indian Ocean sea surface temperature on developing El Niño[J]. Journal of Climate, 2005, 18(2): 302-319.

[12] Izumo T, Vialard J, Lengaigne M, et al. Influence of the state of the Indian Ocean Dipole on the following year's El Niño. Nat Geosci, 2010, 3(3): 168-172.

[13] Wang Lijuan, Chen Shuang, Zhang Haiyan. Characteristics of Southern India Ocean Dipole variation and its relationship with ENSO events[J]. Transactions of Atmospheric Sciences, 2018, 41(3): 344-354.

[14] Fauchereau N, Trzaska S, Richard Y, et al. Sea surface temperature covariability in the southern Atlantic and Indian Oceans and its connections with the atmospheric circulation in the Southern hemisphere[J]. International Journal of Climatology, 2003, 23(6): 663-677.

[15] Penland C, Matrasova L. Studies of El Niño and interdecadal variability in tropical sea surface temperatures using a nonnormal filter[J]. Journal of Climate, 2006, 19(22): 5796-5815.

[16] Penland C, Matrasova L. A Southern Hemisphere footprint in American Midwest precipitation[J]. Geophys Res Lett, 2008, 35(9): L09703.

[17] Wang C. An overlooked feature of tropical climate: inter Pacific-Atlantic variability[J]. Geophys Res Lett, 2006, 33(12): L12702.

[18] Jansen M F, Dommenget D, Keenlyside N. Tropical atmosphere-ocean interactions in a conceptual framework[J]. Journal of Climate, 2009, 22(3): 550-567.

[19] Liu Tingting, Zhang Hua. Comparison between principal component analysis and empirical orthogonal function decomposition[J]. Statistics and Decision making, 2011(16): 159-162.

[20] Yan Chao, Lu Xiaoqing, Zheng Qin. The Mathematical Unification of EOF, SVD and POD[J]. Journal of Mathematics in Practice and Theory, 2014, 44(22): 236-242.

[21] Shi Neng, Wei Fengying, Feng Guolin, et al. Monte Carlo Test used in Correlation and Composite analysis of meteorological fields[J]. Journal of Nanjing Institute of Meteorology, 1997(03): 88-92.

[22] Morioka Y, Ratnam J V, Sasaki W, et al. Generation mechanism of the South Pacific Subtropical Dipole[J]. Journal of Climate, 2013, 26(16): 6033-6045.

[23] Shen Duhan, Lin Xiaopei. The Interannual Variability of the South Atlantic Subtropical Dipole[J]. Journal of Ocean University of China, 2020, 50(01): 1-10.

[24] Li Qiong, Zheng Jian, Wang Faming. Influence of the South Pacific Subtropical Dipole on the South Pacific Convergence Zone[J]. Marine Scieneces, 2016, 40(10): 143-150.

[25] Yuanhong Guan, Bohua Huang, Jieshun Zhu, et al. Interannual variability of the South Pacific Ocean in observations and simulated by the NCEP Climate Forecast System, version 2[J]. Climate Dynamics, 2014, 43(3-4): 1141-1157.